

See discussions, stats, and author profiles for this publication at: <https://www.researchgate.net/publication/231458034>

# Structural studies of copper(I) binding by hydrotris(1-pyrazolyl)borate and hydrotris(3,5-dimethyl-1-pyrazolyl)borate in the solid state and in solution

ARTICLE in JOURNAL OF THE AMERICAN CHEMICAL SOCIETY · FEBRUARY 1976

Impact Factor: 12.11 · DOI: 10.1021/ja00419a012

---

CITATIONS

119

---

READS

4

5 AUTHORS, INCLUDING:



Carlo Mealli

Italian National Research Council

245 PUBLICATIONS 5,037 CITATIONS

SEE PROFILE

# Structural Studies of Copper(I) Binding by Hydrotris(1-pyrazolyl)borate and Hydrotris(3,5-dimethyl-1-pyrazolyl)borate in the Solid State and in Solution

Carlo Mealli,<sup>1</sup> Cathy S. Arcus, Joseph L. Wilkinson, Tobin J. Marks,<sup>\*2</sup> and James A. Ibers\*

Contribution from the Department of Chemistry, Northwestern University, Evanston, Illinois 60201. Received April 18, 1975

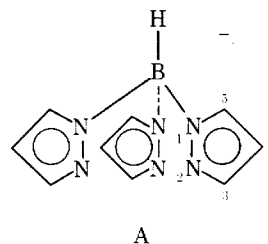
**Abstract:** This contribution presents a detailed comparison of solid-state and solution structural properties for bis[(hydrotris(1-pyrazolyl)borato)copper(I)] ([HBpz<sub>3</sub>Cu]<sub>2</sub>) and bis[(hydrotris(3,5-dimethyl-1-pyrazolyl)borato)copper(I)] ([HB(3,5-Me<sub>2</sub>pz)<sub>3</sub>Cu]<sub>2</sub>). The former compound crystallizes in the triclinic space group  $P\bar{1}$ , with one dimeric molecule in a unit cell of dimensions  $a = 9.264$  (1) Å,  $b = 7.638$  (1) Å, and  $c = 8.181$  (1) Å,  $\alpha = 92.96$  (1)°,  $\beta = 101.71$  (1)°, and  $\gamma = 89.40$  (1)°. Full-matrix least-squares refinement gave a final value of the conventional  $R$  factor (on  $F$ ) of 0.037 for 2111 reflections having  $F^2 > 3\sigma(F^2)$ . The structure consists of discrete centrosymmetric dimeric molecules, with each HBpz<sub>3</sub> ligand presenting a terminally bonded pyrazole ligand to each of the two copper atoms in the dimer ( $\text{Cu-N(av)} = 1.947$  (2) Å), and a symmetrically bridging pyrazole to both copper atoms ( $\text{Cu-N(av)} = 2.239$  (2) Å). The copper-copper distance is 2.660 (1) Å. The complex [HB(3,5-Me<sub>2</sub>pz)<sub>3</sub>Cu]<sub>2</sub> crystallizes in the triclinic space group  $P\bar{1}$  with one molecule in a cell of dimensions  $a = 10.245$  (4) Å,  $b = 10.694$  (3) Å,  $c = 10.034$  (3) Å,  $\alpha = 115.94$  (1)°,  $\beta = 112.13$  (1)°, and  $\gamma = 94.34$  (1)°. Full-matrix least-squares refinement gave a final conventional  $R$  factor (on  $F$ ) of 0.047 for 2786 unique reflections with  $F^2 > 3\sigma(F^2)$ . The structure consists of centrosymmetric dimeric molecules with each HB(3,5-Me<sub>2</sub>pz)<sub>3</sub> ligand presenting two terminally bonded pyrazole units to one copper atom, and one to the other copper atom of the dimer ( $\text{Cu-N(av)} = 1.986$  (3) Å). Any pyrazole bridging interaction is minimal. The copper-copper distance is 2.506 (1) Å. In both [HBpz<sub>3</sub>Cu]<sub>2</sub> and in [HB(3,5-Me<sub>2</sub>pz)<sub>3</sub>Cu]<sub>2</sub>, the major distortion of the ligand from  $C_{3v}$  local symmetry involves twisting about the B-N bonds. In solution, [HBpz<sub>3</sub>Cu]<sub>2</sub> is dimeric. All pyrazole rings are equivalent in the <sup>1</sup>H NMR spectrum down to -130°. The methylated analogue is extensively dissociated in solution. These results imply that pairs of Cu(I) ions in protein polyimidazole binding sites may exhibit high conformational mobility and considerable variation in coordination geometry. Short copper-copper contacts and bridging by imidazole ligands are also conceivable.

A number of metalloproteins are known which contain copper,<sup>3</sup> and which activate molecular dioxygen. These proteins serve the function of dioxygen carriers (hemocyanin)<sup>4</sup> or, more frequently, employ the dioxygen catalytically to oxygenate (oxygenases)<sup>5</sup> or to oxidize (oxidases)<sup>5</sup> organic substrates or other proteins. The actual chemical behavior of many of these copper proteins is well understood in terms of overall reaction stoichiometry. In addition it has been possible to classify the copper in terms of unique EPR (normal A<sub>||</sub>, abnormal A<sub>||</sub>, non-EPR active) and uv-visible (normal, "blue", and colorless) spectral parameters. However, very little is known about the actual ligation sphere of the copper. Without some knowledge of ligands, coordination number, and coordination geometry, as well as analogue chemistry, it is impossible to understand the functional nature of these proteins in any detail. The purpose of this work has been to explore the coordination chemistry of synthetic ligand systems which we believe may be facsimiles of copper chelation sites in these proteins. The goal is to learn how certain natural ligands can impart unique chemical properties, such as reversible dioxygen binding, to copper.

Hemocyanin<sup>4</sup> is a high molecular weight dioxygen-carrying protein found in the blood of arthropods and molluscs. A large body of data suggests it binds one O<sub>2</sub> per two copper subunit; the deoxy form is probably Cu(I) (colorless, diamagnetic) whereas the blue oxy form (with a unique visible spectrum) is probably Cu(II). The coppers are coupled strongly enough to preclude observation of an EPR spectrum. The O-O stretching frequency in oxyhemocyanin suggests oxygen may be present as a peroxide, O<sub>2</sub><sup>2-</sup>.<sup>6</sup> Also, histidine (imidazole) is strongly implicated in copper binding,<sup>4</sup> possibly as the only ligand.<sup>7</sup> With carbon monoxide, hemocyanin forms a carbonyl (1CO/2Cu). The  $\nu_{\text{CO}}$  of 2060–2040 cm<sup>-1</sup><sup>8</sup> is unusually low for a copper carbonyl.<sup>9</sup>

Hemocyanin, we believe, may be a key to understanding the constitution of non-EPR active two-copper units present in many of the copper-containing, dioxygen-activating proteins. For example, it has recently become apparent that hemocyanin is chemically very similar to the oxygenase tyrosinase.<sup>5a-c</sup>

Diffraction studies have now elucidated the geometries of histidine (imidazole) chelating sites in several metalloproteins, viz. human carbonic anhydrase C<sup>10</sup> and B,<sup>11</sup> the two-zinc hexamer of insulin,<sup>12</sup> bovine superoxide dismutase,<sup>13</sup> and carboxypeptidase A $\alpha$ .<sup>14,15</sup> These structural results have led us to examine the anionic hydrotris(1-pyrazolyl)borate ligand<sup>16</sup> (A) (HBpz<sub>3</sub><sup>-</sup>) as an initial approximation of a



multidentate copper binding site. The observation<sup>17</sup> that HBpz<sub>3</sub>Cu is dimeric in solution, and reacts with carbon monoxide to form a stable carbonyl complex with  $\nu_{\text{CO}}$  (2083 cm<sup>-1</sup>) nearly as low as in carboxyhemocyanin, has prompted our chemical and structural investigation of this and related copper pyrazolylborates.<sup>18</sup> In this paper we examine and compare, in detail, the solid-state and solution molecular structures of bis[(hydrotris(1-pyrazolyl)borato)copper(I)] ([HBpz<sub>3</sub>Cu]<sub>2</sub>) and the methylated analogue, bis[hydrotris(3,5-dimethyl-1-pyrazolyl)borato)copper(I)] ([HB(3,5-Me<sub>2</sub>pz)<sub>3</sub>Cu]<sub>2</sub>), to assess the geometrical con-

straints and conformational mobility resulting from the binding of polydentate nitrogen heterocyclic ligands to pairs of interacting Cu(I) ions. The methylated pyrazolylborate complex is of special interest since it forms a carbonyl with  $\nu_{\text{CO}}$  (2066  $\text{cm}^{-1}$ ) even closer to that of carboxyhemocyanin than the unmethylated analogue. We also provide here improved syntheses for the above compounds. The discussion of oxygenation and related redox chemistry as well as other reactions will be deferred to a later contribution.<sup>19</sup>

## Experimental Section

The synthesis and handling of all copper complexes was carried out in an atmosphere of prepurified nitrogen, employing Schlenk apparatus or a glove box. The solid copper pyrazolylborates can be handled in air for brief periods of time without apparent oxidation; however, solutions are considerably more air-sensitive. All common solvents were thoroughly dried and deoxygenated in a manner appropriate to each, and were distilled under nitrogen immediately prior to use. The ligands  $\text{HBpz}_3\text{-K}^+$  and  $\text{HB(3,5-Me}_2\text{pz)}_3\text{-K}^+$  were prepared by the procedure of Trofimenko.<sup>20</sup> Anhydrous cuprous chloride, stated to be 99.999% pure, was obtained from Rocky Mountain Research, Inc. Microanalyses were performed by Miss H. Beck, Northwestern University Analytical Services Laboratory.

**Bis(hydrotris(1-pyrazolyl)borato)copper(I).** Into a three-necked flask under nitrogen were weighed 2.62 g (26.5 mmol) of CuCl and 6.67 g (26.5 mmol) of  $\text{HBpz}_3\text{K}$ . To this solid mixture was added 80 ml of benzene and 130 ml of degassed, deionized water. The mixture was then stirred for 3 h while slowly bubbling carbon monoxide through it. After this time, the pale blue benzene layer was siphoned off, and the aqueous layer extracted with 100 ml more benzene. The combined benzene extracts were dried under nitrogen over anhydrous  $\text{Na}_2\text{SO}_4$ , and were then suction-filtered through a Schlenk frit. The pale blue filtrate was next evaporated under high vacuum to yield 4.2 g (57%) of white, microcrystalline  $[\text{HBpz}_3\text{Cu}]_2$ , mp 150–170° dec. A slightly purer product can be obtained by subsequent Soxhlet extraction with hexane or recrystallization from toluene–pentane at –30°. Note that the carbonyl  $\text{HBpz}_3\text{Cu(CO)}$  is not obtained upon evaporation of the solvent; it could, however, be detected in the infrared spectra of the reaction mixture benzene layer ( $\nu_{\text{CO}} = 2083 \text{ cm}^{-1}$ ). Infrared spectrum ( $\text{cm}^{-1}$ ): 2441 s, 2406 m, 1758 w, 1715 m, 1600 w, 1513 s, 1430 s, 1403 vs, 1388 vs, 1300 vs, 1292 vs, 1226 vs, 1217 vs, 1201 s, 1195 vs, 1130 vs, 1122 vs, 1096 s, 1080 m, 1072 s, 1060 vs, 1050 vs, 988 w, 980 w, 970 m, 922 w, 876 w, 797 w, 761 vs, 755 vs, 729 vs, 721 vs, 666 s, 620 m, 615 m; Raman spectrum ( $\text{cm}^{-1}$ ): 2440 ww, 2267 w, 1980 w, 1968 w, 1431 w, 1406 s, 1391 s, 1299 vs, 1230 s, 1214 vs, 1191 s, 1101 m, 1085 m, 1053 m, 986 w 974 m, 926 s, 781 w, 336 m, 325 w.

Anal. Calcd for  $\text{C}_{18}\text{H}_{20}\text{B}_2\text{Cu}_2\text{N}_{12}$ : C, 39.20; H, 3.63; N, 30.49. Found: C, 39.75; H, 4.28; N, 30.80.

**Hydrotris(3,5-dimethyl-1-pyrazolyl)borato(carbonyl)copper(I).** The above procedure was employed with 1.44 g (15.0 mmol) of CuCl and 4.54 g (15.0 mmol) of  $\text{HB(3,5-Me}_2\text{pz)}_3\text{K}$ . Evaporation of the dried benzene extract yielded 4.08 g (70%) of white, microcrystalline  $\text{HB(3,5-Me}_2\text{pz)}_3\text{Cu(CO)}$ , mp 186–190° dec. Infrared spectrum ( $\text{cm}^{-1}$ ): 2500 m, 2060 vs, 1600 w, 1535 vs, 1450 vs, 1410 sh, 1370 s, 1340 vs, 1195 vs, 1175 vs, 1080 m, 1060 s, 983 m, 853 w, 835 m, 805 vs, 790 vs, 692 s, 641 s.

Anal. Calcd for  $\text{C}_{16}\text{H}_{22}\text{BCuN}_6\text{O}$ : C, 49.44; H, 5.66; N, 21.63. Found: C, 48.23; H, 6.20; N, 21.15.

**Bis(hydrotris(3,5-dimethyl-1-pyrazolyl)borato)copper(I).** Heating finely powdered  $\text{HB(3,5-Me}_2\text{pz)}_3\text{Cu(CO)}$  at 65°C under high vacuum resulted in gradual diminution of  $\nu_{\text{CO}}$  in the infrared spectrum. After 1 week,  $\nu_{\text{CO}}$  was absent. The white solid,  $[\text{HB(3,5-Me}_2\text{pz)}_3\text{Cu}]_2$ , which is obtained by this procedure, mp 186–190° dec, is sufficiently pure for most purposes. A purer product can be obtained by recrystallization from toluene–hexane or  $\text{CH}_2\text{Cl}_2$ –hexane at –30°. Infrared spectrum ( $\text{cm}^{-1}$ ): 2510 m, 1535 s, 1440 vs, 1410 s, 1395 s, 1345 s, 1265 m, 1208 s, 1200 s, 1178 vs, 1080 s, 1040 ms, 985 m, 837 w, 820 s, 810 s, 793 vs, 700 m, 695 m, 655 m, 640 s.

Anal. Calcd for  $\text{C}_{30}\text{H}_{22}\text{B}_2\text{Cu}_2\text{N}_{12}$ : C, 49.93; H, 6.16; N, 23.20. Found: C, 49.88; H, 6.30; N, 22.81.

**Molecular Weight Determinations.** Cryoscopic molecular weights in benzene were determined with the apparatus described previously,<sup>21</sup> or were performed by Dornis and Kolbe (Mulheim). Within experimental error, results on the same compound were identical from the two sources, though the solution concentrations were not available for the latter.

**Spectroscopic Measurements.** Infrared spectra were recorded as Nujol mulls on Beckman IR-5, IR-9, or Perkin-Elmer 267 spectrophotometers, and were calibrated with polystyrene film. Raman spectra were recorded with  $\text{Kr}^+$  (6471 Å) excitation using a Spex 1401 monochromator and photon counting detection. Samples were examined as solids in spinning (1800 rpm) 12-mm Pyrex tubes.

Routine proton NMR spectra at 60 MHz were recorded on Varian T-60 and Perkin-Elmer R20B spectrometers, using serum-capped sample tubes and degassed solvents. Low-temperature studies were performed at 90 MHz on a Bruker HFX-90 instrument. Temperatures were calibrated with a Wilmad thermometer. The solvents  $(\text{CH}_3)_2\text{O}$  and  $\text{CF}_2\text{Cl}_2$  were handled on a vacuum line; they were passed through a –78° trap of molecular sieves and freeze-thaw degassed before distilling into the sample tube, which was then sealed under high vacuum.

**X Ray Study of  $[\text{HBpz}_3\text{Cu}]_2$ .** Crystals suitable for diffraction were grown by slow cooling of a 1/1 toluene–hexane solution of the title compound to –20°. After 1 week at this temperature, the supernatant liquid was withdrawn with a syringe, and the crystals dried under a stream of nitrogen. Preliminary photographic studies showed the colorless crystals of  $[\text{HBpz}_3\text{Cu}]_2$  to lack symmetry and hence be triclinic. Unit cell dimensions were obtained from the centering of 15 reflections on a Picker FACS-1 automated diffractometer using techniques described previously.<sup>22</sup> The  $2\theta$  values for these reflections were in the range 50–60° ( $\text{Cu K}\alpha_1$ ). Based on  $\lambda(\text{Cu K}\alpha_1) = 1.54056 \text{ Å}$ , the dimensions of the reduced cell are  $a = 9.264 (1) \text{ Å}$ ,  $b = 7.638 (1) \text{ Å}$ ,  $c = 8.181 (1) \text{ Å}$ ,  $\alpha = 92.96 (1)^\circ$ ,  $\beta = 101.71 (1)^\circ$ , and  $\gamma = 89.40 (1)^\circ$  at 24.5°C. The calculated density for one dimeric formula unit in the unit cell is 1.626  $\text{g/cm}^3$ . The experimental density, obtained by flotation methods using a solution of  $\text{ZnCl}_2$ , is 1.58 (2)  $\text{g/cm}^3$ . The crystal selected for data collection was of equant habit with approximate overall dimensions 0.24 × 0.26 × 0.28 mm. The crystal showed faces of the forms  $\{100\}$ ,  $\{010\}$ ,  $\{001\}$ ,  $\{10\bar{1}\}$ , and in addition, the face  $\{1\bar{1}1\}$ . The calculated volume of the crystal is 0.0175  $\text{mm}^3$ . Intensity data were collected using prefiltered (Ni foil, 1 mil) Cu radiation. The take off angle of 3° gave 85% of the maximum Bragg intensity available for a given reflection. The crystal to counter distance was 32.0 cm and the aperture was 4.0 mm wide by 5.0 mm high. The  $\theta$ – $2\theta$  scan technique was employed, with a scan range of 2.0° corrected for dispersion at a rate of 2.0°  $\text{min}^{-1}$ . Background counts were made for 10 s with a stationary crystal and counter at the end of each scan. Background time was increased to 20 s for  $2\theta > 140^\circ$ . Coincidence losses were minimized for strong reflections by employing copper foil attenuators (ratio = 2.3).

A total of 2455 reflections covered the reciprocal hemisphere, for which  $k$  was negative, up to a  $2\theta$  value of 160°. Starting at  $2\theta = 125^\circ$ , the parallel mode was used for collection. In the bisecting mode, the intensity of six reflections in diverse regions of reciprocal space were monitored every 100 reflections; in the parallel mode three such reflections were monitored. The variation in an individual standard was less than that expected from counting statistics. Data were processed in the usual way,<sup>22</sup> with  $p = 0.03$ . The values of  $I$  and  $\sigma(I)$  were corrected for Lorentz, polarization, and absorption effects, thereby yielding 2111 unique reflections with  $F^2 \geq 3\sigma(F^2)$ . Transmission factors ranged from 0.506 to 0.610 using a linear absorption coefficient for Cu  $K\alpha$  radiation of 25.62  $\text{cm}^{-1}$ .

A Patterson map was used to locate the positions of the copper atoms and all of the six nitrogen atoms present in the asymmetric unit. It was clear at this point that the molecule is a centrosymmetric dimer. The carbon atoms were found in a subsequent  $F_o$  Fourier synthesis. Refinement of the structure was by full-matrix least-squares methods. The procedures and sources of atomic scattering factors have been reported elsewhere.<sup>23</sup> The course of refinement, as indicated by values of  $R$  and  $R_w$  in parentheses, was as follows: complete isotropic refinement of all the 17 non-hydrogen atoms (0.115, 0.182); three cycles of anisotropic refinement including a fixed contribution for the ten hydrogen atoms and an isotropic extinction parameter (0.037, 0.066). The pyrazole ring C–H dis-

**Table I.** Positional and Thermal Parameters for the Atoms of [HBpz<sub>3</sub>Cu]<sub>2</sub>

Atom	<i>x</i> <sup>a</sup>	<i>y</i>	<i>z</i>	<i>B</i> <sub>11</sub> <sup>b</sup>	<i>B</i> <sub>22</sub>	<i>B</i> <sub>33</sub>	<i>B</i> <sub>12</sub>	<i>B</i> <sub>13</sub>	<i>B</i> <sub>23</sub>
Cu	0.03695(4)	-0.15174(5)	-0.06762(5)	83.4(6)	164.2(12)	130.5(8)	14.8(5)	-9.0(5)	3.5(6)
N1	0.24783(24)	-0.1869(3)	0.00794(28)	85.7(26)	150.(4)	116.(3)	22.9(26)	7.6(23)	-5.2(28)
N3	0.14543(24)	0.25825(29)	0.19167(27)	94.1(27)	110.(4)	116.(3)	9.8(24)	-1.1(23)	9.4(27)
N5	-0.00329(23)	-0.1011(3)	0.19331(29)	69.5(24)	170.(5)	130.(3)	-7.9(25)	6.8(23)	25.(3)
N2	0.32786(22)	-0.12584(27)	0.15806(26)	70.1(23)	104.(4)	118.(3)	9.4(22)	11.0(21)	10.9(26)
N4	0.25850(22)	0.16927(27)	0.28559(25)	71.6(23)	104.(4)	101.8(29)	-0.6(22)	9.1(20)	3.5(25)
N6	0.11953(22)	-0.11037(27)	0.31708(24)	79.2(23)	110.(4)	93.5(28)	6.0(22)	14.4(20)	14.1(24)
B	0.26746(28)	-0.0327(4)	0.3024(3)	71.1(28)	110.(5)	104.(4)	7.0(28)	5.2(25)	16.(3)
C1	0.3434(3)	-0.2632(4)	-0.0750(4)	117.(4)	182.(6)	141.(5)	43.(4)	26.(3)	-9.(4)
C2	0.4849(3)	-0.2530(5)	0.0175(4)	96.(3)	205.(7)	181.(5)	31.(4)	47.(3)	5.(5)
C3	0.47117(28)	-0.1650(4)	0.1644(4)	71.5(29)	169.(6)	159.(5)	12.(3)	18.3(28)	14.(4)
C4	0.1834(4)	0.4256(4)	0.2099(4)	134.(4)	167.(5)	150.(5)	13.(3)	23.(3)	17.(4)
C5	0.3203(4)	0.4490(4)	0.3145(4)	127.(4)	120.(5)	189.(5)	-29.(4)	20.(4)	-4.(4)
C6	0.3628(3)	0.2930(4)	0.3609(4)	88.(3)	154.(6)	141.(4)	-21.(3)	12.4(28)	-3.(4)
C7	-0.1086(3)	-0.1871(4)	0.2457(4)	89.(3)	190.(6)	180.(5)	-24.(3)	50.(3)	-13.(4)
C8	-0.0559(4)	-0.2511(4)	0.4020(4)	141.(4)	153.(6)	184.(5)	-21.(4)	89.(4)	10.(4)
C9	0.0876(4)	-0.2002(4)	0.4426(3)	142.(4)	123.(5)	121.(4)	4.(3)	46.(3)	24.(3)

<sup>a</sup> Estimated standard deviations in the least significant figure(s) are given in parentheses in this and all subsequent tables. <sup>b</sup> The form of the anisotropic thermal ellipsoid is:  $\exp[-(B_{11}h^2 + B_{22}k^2 + B_{33}l^2 + 2B_{12}hk + 2B_{13}hl + 2B_{23}kl)]$ . The quantities given in the table are the thermal coefficients  $\times 10^4$ .

tances were assumed to be 0.95 Å, whereas the B-H distance was fixed at 1.00 Å. The isotropic thermal parameters of the hydrogen atoms were fixed 1 Å<sup>2</sup> greater than those of their bonded carbon atoms. The standard deviation of an observation of unit weight is 3.64 e. The value of the extinction parameter is  $2.5(2) \times 10^{-6} \text{ e}^{-2}$ . A final difference Fourier map shows no peak higher than 0.4 e/Å, except for a peak at the origin of the cell with an electron density of 1.2 e/Å; this point is also the center of symmetry of the dimer. Analysis of  $\Sigma w(|F_o| - |F_c|)^2$  as a function of Miller indices,  $|F_o|$ , and diffractometer setting angles, revealed no particular trends. The positional and thermal parameters obtained from the last cycle of least-squares refinement are given in Table I along with their standard deviations as estimated from the inverse matrix. Calculated positions of the hydrogen atoms are given in Table II.<sup>24</sup> Root-mean-square amplitudes of vibration are given in Table III.<sup>24</sup> Tables II and III, and final values of  $100|F_o|$  and  $100|F_c|$  in electrons will appear in the microfilm edition.<sup>24</sup>

**X Ray Study of [HB(3,5-Me<sub>2</sub>pz)<sub>3</sub>Cu]<sub>2</sub>.** Crystals were grown by dissolving the title compound in CH<sub>2</sub>Cl<sub>2</sub>, adding pentane until cloudiness, and slowly cooling to -20°. After 3 days, the crystals were collected by removing the supernatant via syringe and drying them under a stream of nitrogen. Photographs of one of these colorless prisms with dimensions 0.09 × 0.26 × 0.29 mm revealed no symmetry other than the center of inversion. A set of 15 reflections in the 2θ range of 50–60° (Cu Kα, λ 1.540562 Å), was centered on a Picker FACS-1 automatic diffractometer. The lattice dimensions for the reduced triclinic cell are *a* = 10.245 (4) Å, *b* = 10.694 (3) Å, *c* = 10.034 (3) Å, α = 115.94 (1)°, β = 112.13 (1)°, γ = 94.34 (1)°, and *V* = 876.75 Å<sup>3</sup> at 23°C. The calculated density for one dimeric formula unit in the cell is 1.367 g/cm<sup>3</sup>. No experimental density was measured, because the crystals are soluble in most common organic solvents, and strong surface tension effects take place when the flotation method is attempted in aqueous solutions of ZnCl<sub>2</sub>.

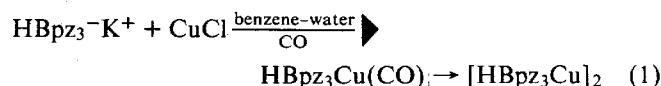
Data were collected as described above for the unmethylated complex. Differences were: the takeoff angle was 3.6°; the aperture was 4.5 mm high by 5.5 mm wide; background counts were made for 10 s up to 2θ = 93°; beyond this limit the time was increased to 20 s. A total of 3775 reflections (*h* < 0) was examined out to 2θ = 160°. The data were processed in the normal manner,<sup>22</sup> with *p* = 0.03, including a small correction for the observed 4% decrease in the intensities of the standards during data collection. An absorption correction was also applied. The transmission factors fell in the range 0.646–0.886 using a linear absorption coefficient for Cu Kα radiation of 17.68 cm<sup>-1</sup>. For structure solution and refinement 2786 unique reflections with *F*<sup>2</sup> > 3σ(*F*<sup>2</sup>) were used.

A three-dimensional Patterson map followed by a difference Fourier located the positions of all non-hydrogen atoms. Refinement of the structure was then begun by full-matrix least-squares

methods. Three isotropic cycles for all of the 23 non-hydrogen atoms gave *R* = 0.159 and *R*<sub>w</sub> = 0.203. Three anisotropic cycles, the second and third one including a fixed contribution from the hydrogen atoms, led to the final values *R* = 0.047 and *R*<sub>w</sub> = 0.064. Twenty of the twenty-two hydrogen atoms in the asymmetric unit were located in a difference Fourier map calculated after the first anisotropic cycle. However, they were introduced in the following calculations assuming ideal positions for them (B-H = 1.0 Å, C-H = 0.95 Å (aromatic pyrazole carbon), C-H = 1.0 Å (methyl carbon)), the positions for those belonging to the methyl groups being determined by a least-squares adjustment to observed positions. The error in an observation of unit weight is 2.08 e<sup>-</sup>. Positional and thermal parameters obtained from the final cycle of refinement are given in Table IV, together with associated standard deviations as estimated from the inverse matrix. Calculated hydrogen atom positions appear in Table V,<sup>24</sup> and root-mean-square amplitudes of vibration in Table VI.<sup>24</sup> Tables V and VI as well as final values of  $100|F_o|$  and  $100|F_c|$  will appear in the microfilm edition.<sup>24</sup>

## Results

**Synthesis.** The compound [HBpz<sub>3</sub>Cu]<sub>2</sub> was prepared via the carbonyl, HBpz<sub>3</sub>Cu(CO), in a variant of the literature procedure,<sup>17</sup> eq 1.

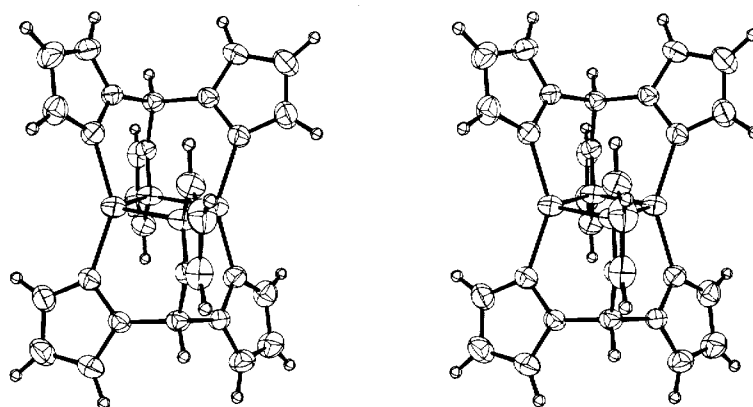
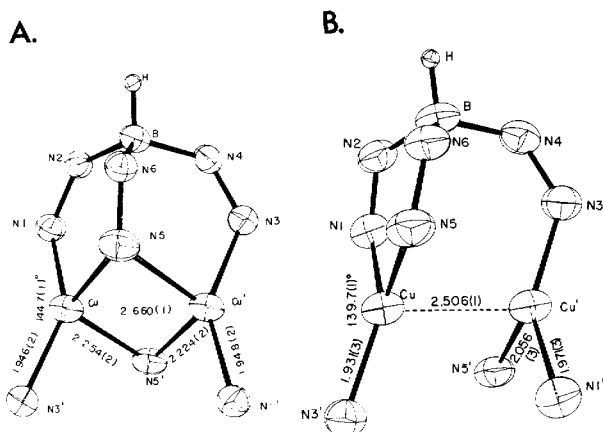


The two-phase reaction system produces a cleaner, more readily isolable product in relatively high yield. The use of very pure (99.999%) CuCl greatly reduces contamination by Cu(II) products such as (HBpz<sub>3</sub>)<sub>2</sub>Cu. Though the intermediate carbonyl could be detected in reaction solutions by infrared spectroscopy, evaporation of the solvent invariably yielded decarbonylated product, [HBpz<sub>3</sub>Cu]<sub>2</sub>. When eq 1 was carried out with HB(3,5-Me<sub>2</sub>pz)<sub>3</sub>K<sup>+</sup>,<sup>20</sup> the product isolated was the carbonyl, HB(3,5-Me<sub>2</sub>pz)<sub>3</sub>Cu(CO).<sup>17</sup> This was only decarbonylated on prolonged heating and pumping, to yield the new compound, [HB(3,5-Me<sub>2</sub>pz)<sub>3</sub>Cu]<sub>2</sub>. The copper carbonyl with methylated pyrazole rings is considerably less labile. The reasons appear to be both electronic (*ν*<sub>CO</sub> = 2066 vs. 2083 cm<sup>-1</sup>) and steric (vide infra).

**[HBpz<sub>3</sub>Cu]<sub>2</sub> Crystal Structure Description.** The solid-state structure of this compound consists of neutral dimeric molecules, one per unit cell. The intermolecular contacts

Table IV. Positional and Thermal Parameters for the Atoms of  $[\text{HB}(\text{Me}_2\text{pz})_3\text{Cu}]_2$ 

Atom	x	y	z	$B_{11}$	$B_{22}$	$B_{33}$	$B_{12}$	$B_{13}$	$B_{23}$
Cu	0.069894 (65)	-0.054706 (62)	0.081797 (65)	189.8 (10)	180.10 (90)	178.5 (10)	102.27 (74)	134.73 (83)	111.61 (77)
N(1)	-0.13415 (33)	-0.10835 (32)	-0.30879 (35)	139.1 (42)	147.8 (40)	158.0 (47)	53.2 (33)	87.8 (38)	86.8 (37)
N(2)	-0.03408 (30)	-0.13310 (29)	-0.37068 (30)	122.6 (37)	125.9 (35)	114.2 (38)	34.6 (29)	68.1 (32)	58.7 (30)
N(3)	0.14956 (30)	-0.18858 (28)	-0.04652 (33)	128.0 (39)	114.1 (33)	161.4 (46)	48.8 (30)	88.9 (36)	71.6 (33)
N(4)	0.15215 (29)	-0.21524 (27)	-0.19271 (32)	117.8 (37)	102.4 (31)	136.6 (40)	43.4 (28)	74.7 (33)	43.2 (30)
N(5)	0.14670 (32)	0.12786 (28)	-0.02267 (32)	148.3 (42)	111.1 (34)	136.0 (41)	42.1 (31)	91.2 (36)	51.0 (32)
N(6)	0.20762 (29)	0.04769 (27)	-0.12098 (30)	118.4 (37)	111.9 (32)	129.1 (39)	37.0 (28)	78.8 (32)	55.7 (30)
B	0.12953 (43)	-0.11036 (40)	-0.26301 (43)	132.5 (54)	118.2 (44)	122.2 (51)	36.6 (40)	86.2 (46)	47.0 (40)
C(1)	-0.26660 (42)	-0.15691 (43)	-0.43875 (49)	132.6 (51)	157.4 (51)	205.6 (68)	51.5 (42)	70.4 (50)	112.2 (51)
C(2)	-0.25306 (46)	-0.21056 (43)	-0.58509 (46)	163.0 (60)	154.4 (53)	160.8 (61)	35.8 (46)	41.1 (50)	89.7 (49)
C(3)	-0.10635 (42)	-0.19294 (36)	-0.53894 (39)	171.2 (58)	111.4 (40)	124.4 (48)	29.8 (38)	68.9 (45)	58.2 (37)
C(1M)	-0.40129 (52)	-0.14694 (63)	-0.41282 (69)	146.2 (65)	273.9 (94)	326. (12)	82.8 (65)	102.2 (73)	168.9 (91)
C(2M)	-0.03113 (51)	-0.22418 (43)	-0.64656 (42)	239.2 (75)	156.7 (54)	126.5 (54)	37.0 (51)	107.7 (55)	65.6 (45)
C(4)	0.18672 (41)	-0.29646 (39)	-0.02063 (50)	137.4 (52)	132.9 (46)	229.3 (72)	51.7 (40)	98.1 (52)	106.1 (50)
C(5)	0.21531 (45)	-0.39104 (37)	-0.14618 (52)	156.8 (57)	98.4 (40)	224.0 (74)	47.9 (39)	70.9 (54)	61.9 (46)
C(6)	0.19168 (41)	-0.33936 (38)	-0.25269 (44)	140.6 (53)	114.9 (42)	164.9 (59)	52.2 (39)	71.5 (47)	27.3 (41)
C(3M)	0.19618 (62)	-0.29953 (58)	0.12928 (71)	279.7 (97)	250.3 (85)	370. (12)	143.6 (76)	206.2 (94)	240.5 (92)
C(4M)	0.20606 (61)	-0.40191 (51)	-0.41006 (52)	301. (10)	196.4 (70)	180.6 (71)	145.3 (72)	135.8 (73)	50.6 (58)
C(7)	0.24743 (42)	0.25659 (36)	0.08898 (41)	164.9 (55)	107.5 (39)	141.6 (52)	41.1 (38)	81.7 (46)	59.1 (38)
C(8)	0.37247 (43)	0.26012 (39)	0.06574 (45)	146.2 (54)	122.1 (44)	168.7 (60)	13.2 (40)	66.0 (48)	61.3 (43)
C(9)	0.34475 (38)	0.12650 (38)	-0.06781 (41)	128.0 (48)	134.8 (43)	156.5 (54)	41.8 (37)	77.9 (43)	82.0 (41)
C(5M)	0.21930 (53)	0.37258 (41)	0.21946 (50)	232.7 (77)	113.5 (46)	186.3 (69)	42.2 (48)	117.5 (63)	35.6 (46)
C(6M)	0.44168 (42)	0.06888 (45)	-0.14482 (52)	130.4 (53)	180.6 (59)	229.0 (74)	49.9 (46)	109.9 (54)	102.5 (56)

Figure 1. Stereoscopic view of  $[\text{HBpz}_3\text{Cu}]_2$ . The 50% probability vibrational ellipsoids are shown.Figure 2. (A) Perspective view of the immediate copper coordination sphere in  $[\text{HBpz}_3\text{Cu}]_2$ . (B) Perspective view of the immediate copper coordination sphere in  $[\text{HB}(3,5\text{-Me}_2\text{pz})_3\text{Cu}]_2$ . The 50% probability vibrational ellipsoids are shown.

are normal, the shortest being the N(4)–H(8) (the hydrogen bound to C(8)) distance of 2.87 Å.

A stereoscopic view of a single dimeric molecule is presented in Figure 1. Figure 2A summarizes the important features of the copper coordination geometry and shows the atom numbering scheme. Selected intramolecular bond distances and angles are reported in Table VII. The molecule has a crystallographically imposed center of symmetry, with each  $\text{HBpz}_3$  moiety presenting two terminal pyrazole ligands (one to each copper) and one crosswise bridging pyrazole ligand. Both of the above features of the ligation are unprecedented in pyrazolylborate coordination chemistry.<sup>16</sup> The coordination geometry about each copper atom can be roughly described as a distorted tetrahedron, with the six N–Cu–N bond angles being 144.75 (10), 93.74 (9), 108.20 (9), 104.37 (9), 95.18 (9), and 107.13 (7)°. The terminal pyrazole Cu–N distances are 1.946 (2) and 1.948 (2) Å, while the bridging pyrazole Cu–N distances are appreciably longer, 2.254 (2) and 2.224 (2) Å. It can be seen from these

**Table VII.** Selected Bond Distances (Å) and Angles (deg) [HBpz<sub>3</sub>Cu]<sub>2</sub> vs. [HB(Me<sub>2</sub>pz)<sub>3</sub>Cu]<sub>2</sub><sup>a</sup>

Cu–Cu'	2.660 (1) <sup>b</sup>	2.507 (1) <sup>c</sup>	N(1)–Cu–N(3)'	144.75 (10) <sup>b</sup>	139.66 (11) <sup>c</sup>		
Cu–N(1)	1.946 (2)	1.971 (3)	N(1)–Cu–N(5)	93.74 (9)	97.94 (10)		
Cu–N(3)'	1.948 (2)	1.931 (3)	N(1)–Cu–N(5)'	108.20 (9)			
Cu–N(5)	2.254 (2)	2.056 (3)	N(3)'–Cu–N(5)	104.37 (9)	117.39 (10)		
Cu–N(5)'	2.224 (2)	2.777 (4)	N(3)'–Cu–N(5)'	95.18 (9)			
B–N(2)	1.545 (3)	1.543 (4)	N(5)–Cu–N(5)'	107.13 (7)	112.87 (32)		
B–N(4)	1.556 (3)	1.554 (4)	Cu–N(5)–Cu'	72.87 (6)	111.97 (30)		
B–N(6)	1.528 (3)	1.535 (4)	N(2)–B–N(4)	111.65 (20)	110.25 (27)		
			N(2)–B–N(6)	111.21 (20)			
			N(4)–B–N(6)	111.96 (19)			
			B–N(2)–N(1)	126.73 (20)	123.31 (28)		
			B–N(4)–N(3)	125.99 (19)	124.49 (27)		
			B–N(6)–N(5)	122.36 (19)	123.12 (29)		
Ring 1							
N(1)–N(2)	1.361 (3)	1.372 (5)	N(2)–N(1)–C(1)	106.47 (22)	107.07 (32)	N(1)–C(1)–C(1M)	120.34 (43) <sup>c</sup>
N(1)–C(1)	1.332 (3)	1.334 (4)	N(1)–N(2)–C(3)	108.79 (21)	108.85 (28)	C(2)–C(1)–C(1M)	129.89 (37)
C(1)–C(2)	1.376 (4)	1.391 (5)	N(1)–C(1)–C(2)	111.26 (27)	109.76 (40)	N(2)–C(3)–C(2M)	123.68 (34)
C(2)–C(3)	1.374 (4)	1.366 (6)	C(1)–C(2)–C(3)	104.46 (25)	106.12 (33)	C(2)–C(3)–C(2M)	128.08 (35)
C(3)–N(2)	1.349 (3)	1.360 (4)	C(2)–C(3)–N(2)	109.02 (25)	108.17 (40)		
C(1)–C(1M)		1.501 (6)					
C(3)–C(2M)		1.492 (5)					
Ring 2							
N(3)–N(4)	1.364 (3)	1.378 (5)	N(4)–N(3)–C(4)	106.29 (22)	106.76 (31)	N(3)–C(4)–C(3M)	120.56 (41)
N(3)–C(4)	1.322 (4)	1.341 (6)	N(3)–N(4)–C(6)	109.29 (22)	108.20 (34)	C(5)–C(4)–C(3M)	129.34 (48)
C(4)–C(5)	1.386 (4)	1.380 (6)	N(3)–C(4)–C(5)	111.19 (26)	110.07 (47)	N(4)–C(6)–C(4M)	123.23 (44)
C(5)–C(6)	1.373 (4)	1.359 (7)	C(4)–C(5)–C(6)	104.23 (25)	106.19 (41)	C(5)–C(6)–C(4M)	128.00 (48)
C(6)–N(4)	1.337 (3)	1.362 (5)	C(5)–C(6)–N(4)	108.97 (25)	108.76 (37)		
C(4)–C(3M)		1.485 (6)					
C(6)–C(4M)		1.493 (7)					
Ring 3							
N(5)–N(6)	1.365 (3)	1.379 (4)	N(6)–N(5)–C(7)	105.92 (23)	105.96 (31)	N(5)–C(7)–C(5M)	120.86 (39)
N(5)–C(7)	1.334 (3)	1.334 (4)	N(5)–N(6)–C(9)	109.29 (22)	110.03 (24)	C(8)–C(7)–C(5M)	128.64 (31)
C(7)–C(8)	1.385 (5)	1.387 (7)	N(5)–C(7)–C(8)	110.90 (27)	110.47 (32)	N(6)–C(9)–C(6M)	123.22 (29)
C(8)–C(9)	1.359 (4)	1.376 (5)	C(7)–C(8)–C(9)	104.88 (24)	106.17 (32)	C(8)–C(9)–C(6M)	129.40 (36)
C(9)–N(6)	1.346 (3)	1.353 (5)	C(8)–C(9)–N(6)	109.00 (26)	107.36 (37)		
C(7)–C(5M)		1.501 (6)					
C(9)–C(6M)		1.490 (7)					
Dihedral Angles between Indicated Planes <sup>d</sup>							
HBN(2)–BN(2)N(1)	26.21	2.08					
HBN(4)–BN(4)N(3)	0.62	18.56					
HBN(6)–BN(6)N(5)	21.26	24.10					

<sup>a</sup> See Figures 2 and 3 for atom numbering scheme. <sup>b</sup> Parameters for [HBpz<sub>3</sub>Cu]<sub>2</sub>. <sup>c</sup> Parameters for [HB(Me<sub>2</sub>pz)<sub>3</sub>Cu]<sub>2</sub>. <sup>d</sup> Standard deviations were not calculated owing to the uncertainty in the H positions.

distances that the bridge is only slightly (0.03 Å) unsymmetrical. The copper–copper distance in the dimer is 2.660 (1) Å.

Important bond angles and distances within the hydrotris(1-pyrazolyl)borato ligand are also presented in Table VII. Within experimental error, internal distances and angles for bridging and terminal pyrazole rings are identical. These data are summarized in Figure 3. No atom in a ring deviates from its ring least-squares plane by more than 0.005 Å. Also, bond distances within the HBpz<sub>3</sub> ligand do not differ greatly from complexes in which the HBpz<sub>3</sub> ligand is bound to a single metal, i.e., HBpz<sub>3</sub>Cu(CO),<sup>25</sup> (HBpz<sub>3</sub>)<sub>2</sub>Co,<sup>26</sup> (HBpz<sub>3</sub>)(COCH<sub>3</sub>)Fe(CO)<sub>2</sub>,<sup>27</sup> CH<sub>3</sub>–(HBpz<sub>3</sub>)Pt(CF<sub>3</sub>C≡CCF<sub>3</sub>),<sup>28</sup> and (HBpz<sub>3</sub>)Mo(CO)<sub>2</sub>–(N<sub>2</sub>C<sub>6</sub>H<sub>5</sub>).<sup>29</sup> For example, for the above five structures, the B–N distances range from 1.526 (6) to 1.558 (6) Å vs. 1.543 (3) Å for the present study. Likewise, the intra-ring N–N distances previously determined range from 1.350 (5) to 1.378 (5) Å vs. 1.363 (2) Å for [HBpz<sub>3</sub>Cu]<sub>2</sub>. Furthermore, dimer formation and bridging of the metals has effected only a small perturbation in the boron valence angles. The N–B–N angles (average) for the above five structures fall between 107.1 (4)° and 111.3 (3)°, and the B–N–N angles between 119.2 (5)° and 121.2 (6)°. For the copper pyrazolylborate dimer, the N–B–N angle (average) is 111.6 (5)°, i.e., only 3.6 (7)° greater than the average of the other

five values, and the angle B–N–N is 125.0 (4)° (average), a value 5.2 (1.0)° larger than the average for the five monomeric HBpz<sub>3</sub> complexes. The major distortion suffered by the HBpz<sub>3</sub> ligand on bridging the two copper atoms involves rotation about B–N (ring) bonds. While the previous mononuclear structures have hydrotris(pyrazolyl)borate ligands of approximately C<sub>3v</sub> local symmetry, the HBN plane–ring plane dihedral angles in [HBpz<sub>3</sub>Cu]<sub>2</sub> are 26.2 and 21.3° for the terminal pyrazole rings. The angle for the bridging ring is more normal at 0.6°. The degree of distortion can be readily seen in Figure 4A; numerical data are set out in Table VII.

**[HB(3,5-Me<sub>2</sub>pz)<sub>3</sub>Cu]<sub>2</sub> Crystal Structure Description.** The overall structure of this complex consists of centrosymmetric dimers, with normal intermolecular contacts. The shortest contact not involving hydrogen is that of C(14)–C(10), 3.498 Å, while for contacts involving hydrogen, the shortest is C(4)–H(2), 2.62 Å.

A stereoscopic view of a single dimer is presented in Figure 5. Selected intramolecular bond distances and angles can be found in Table VII. The immediate copper coordination sphere along with the atom numbering system is shown in Figure 2B. As found for the unmethylated analogue, the copper(I) complex of the hydrotris(2,5-dimethyl-1-pyrazolyl)borate ligand has a crystallographically imposed centrosymmetric, dimeric structure. Also, the pyrazolylborate li-

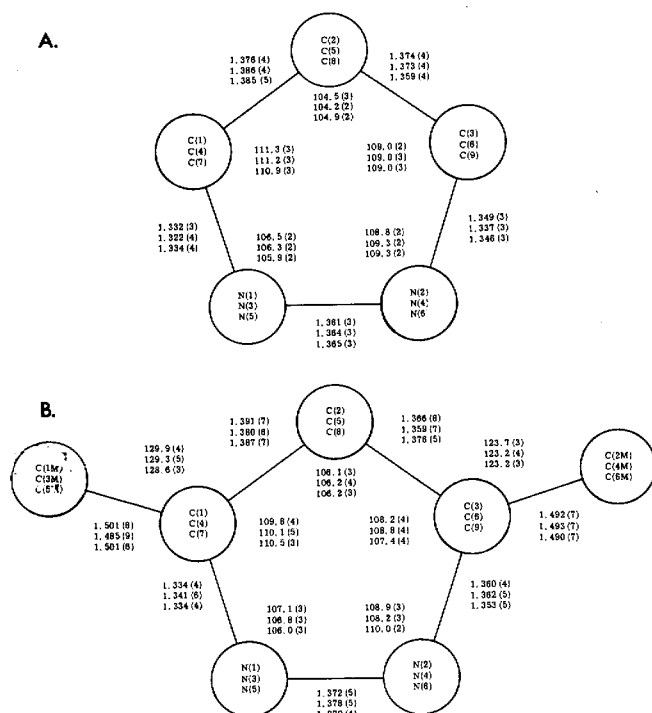


**Figure 3.** (A) Summary of pyrazole ring bond distances and angles in [HBpz<sub>3</sub>Cu]<sub>2</sub>. (B) Summary of pyrazole ring bond distances and angles in [HB(3,5-Me<sub>2</sub>pz)<sub>3</sub>Cu]<sub>2</sub>. Ring parameters are listed vertically in the order of nitrogen atoms contained in that particular ring: N(1)N(2), N(3)N(4), N(5)N(6).

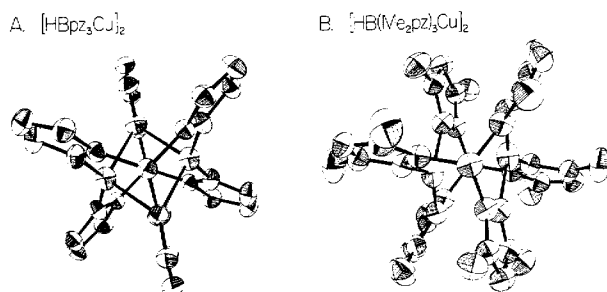


**Figure 4.** (A) Perspective view of [HBpz<sub>3</sub>Cu]<sub>2</sub> along the B-B' bond axis. (B) Perspective view of [HB(3,5-Me<sub>2</sub>pz)<sub>3</sub>Cu]<sub>2</sub> along the B-B' bond axis.

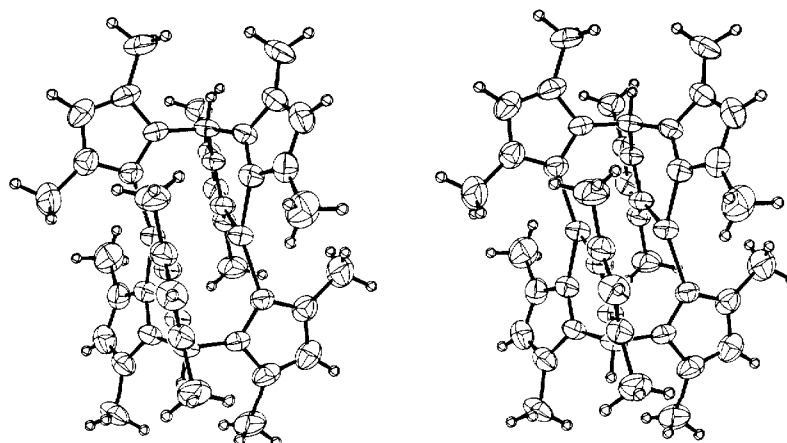


**Figure 5.** Stereoscopic view of [HB(3,5-Me<sub>2</sub>pz)<sub>3</sub>Cu]<sub>2</sub>. The 50% probability vibrational ellipsoids are shown.

gands bridge both copper atoms. Here the similarity in ligation geometry ends, as can be seen most readily in Figure 2, which compares the immediate coordination sphere about the copper atoms in both complexes. A considerable reorganization of the copper coordination geometry has occurred upon introduction of the bulky methyl groups. The molecule now lacks symmetrically bridging pyrazolyl rings, so that the formal coordination number of each copper atom has decreased from four to approximately three. The immediate coordination geometry is best described as distorted trigonal planar, with N-Cu-N angles of 139.66 (11), 97.94 (10), and 117.39 (10)° (Table VII). The copper-nitrogen distances of 1.971 (3) Å (Cu-N(1)), 2.056 (3) Å (Cu-N(5)), and 1.931 (3) Å (Cu-N(3')) are similar to those found for [HBpz<sub>3</sub>Cu]<sub>2</sub>, i.e., 1.974 (2) Å (average). The copper lies only 0.245 Å out of the plane defined by these three nitrogen atoms. The fact that, in the present structure, Cu-N(5) is slightly lengthened over the other two Cu-N distances, and that Cu-N(5) is only 2.777 (4) Å, implies that some residual bridge bonding may be taking place. The copper-copper distance is 2.506 (1) Å, shorter than in the unmethylated complex by 0.154 Å.

The geometry within the HB(2,5-Me<sub>2</sub>pz)<sub>3</sub> ligand is summarized in Table VII. No diffraction studies have been reported for a monomeric HB(2,5-Me<sub>2</sub>pz)<sub>3</sub> complex,<sup>30</sup> so that comparisons are not possible. As can be seen in Table VII, the angles and bond distances within the ligand are quite similar to those in [HBpz<sub>3</sub>Cu]<sub>2</sub>. Thus, dimer formation has done little to alter what appear to be normal boron valence angles and B-N distances. As is summarized in Figure 3B, bond distances and angles within the three dimethylpyrazole rings are virtually identical. The maximum deviation of an atom in a ring from the least-squares plane is 0.009 Å. The maximum deviation of a methyl carbon is 0.097 Å. The principal perturbation in ligand geometry from C<sub>3v</sub> is, as for the case of the unmethylated analogue, in the dihedral angles between the HBN and pyrazole ring planes. These are, for each HB(3,5-Me<sub>2</sub>pz)<sub>3</sub> ligand, 2.1, 18.6, and 24.1° (Table VII), and the twisting about the B-N bonds is readily appreciated in Figure 4B. Again, this heretofore unrecognized mode of distortion allows the pyrazolylborate ligand considerable flexibility in accommodating a pair of Cu(I) ions.

**Solution Studies.** Though the dimeric structures of [HBpz<sub>3</sub>Cu]<sub>2</sub> and [HB(3,5-Me<sub>2</sub>pz)<sub>3</sub>Cu]<sub>2</sub> were established in the solid state, it was of interest to investigate both the integrity and rigidity of these structures in solution. The molecular weight of [HBpz<sub>3</sub>Cu]<sub>2</sub>, determined by osmometry in CHCl<sub>3</sub>, was reported to be that of a dimer.<sup>17</sup> We have verified and supplemented this finding by cryoscopic studies in

benzene: calcd for a dimer, 553; found, 576, 541 (0.004–0.005 M solutions). The proton magnetic resonance spectrum of this complex surprisingly indicates magnetic equivalence of the terminal and bridging pyrazole rings at room temperature. The spectrum (toluene- $d_8$ ) exhibits resonances at  $\tau$  2.42 (3 H, doublet), 2.95 (3 H, doublet), and 4.05 (3 H, triplet). This result indicates (excluding unlikely accidental magnetic degeneracy) that rapid interchange of the two kinds of heterocyclic rings is occurring.  $^1\text{H}$  NMR spectra (90 MHz) were recorded as low as  $-130^\circ$  in dimethyl ether–toluene- $d_8$  mixtures. Though considerable broadening of the spectrum was observed by  $-120^\circ$ , no splitting of peaks could be detected which would indicate proximity to the slow exchange limit. Efforts to reach lower temperatures in Freon solvents were thwarted by the low solubility of this compound. These DNMR results suggest that the activation energy for bridge–terminal ligand interchange in  $[\text{HBpz}_3\text{Cu}]_2$  is very low, i.e., less than or equal to ca. 8 kcal/mol.

The molecular weight of the new compound  $[\text{HB}(3,5\text{-Me}_2\text{pz})_3\text{Cu}]_2$  was also investigated in benzene solution by cryoscopy. Surprisingly, we find it to be extensively dissociated in the 0.005 M concentration region: calcd for a dimer, 722; found, 415, 428. The room temperature proton NMR spectrum (toluene- $d_8$ ) exhibits peaks at  $\tau$  4.30 (3 H, singlet), 7.75 (9 H, singlet), and 8.22 (9 H, singlet). The pyrazolyl rings are again magnetically equivalent. In view of the results for the unmethylated compound and the high level of dissociation in the present case, variable temperature NMR studies were not undertaken.

## Discussion

The objective of the present study was to probe the geometry and mobility of Cu(I) coordination by synthetic ligands which might simulate multiimidazole binding sites in certain metalloproteins. The hydrotris(1-pyrazolyl)borate ligand and its 3,5-dimethylpyrazolyl analogue were chosen as crude initial facsimiles, since the Cu(I) complex of the former bears some chemical and spectroscopic similarity to hemocyanin.<sup>18,19</sup> It is of interest to discuss our structural results on  $[\text{HBpz}_3\text{Cu}]_2$  and  $[\text{HB}(3,5\text{-Me}_2\text{pz})_3\text{Cu}]_2$  in light of results for other Cu(I) complexes with nitrogenous ligands. Unfortunately, there is little crystallographic data available for Cu(I) complexes of naturally occurring nitrogenous ligands.<sup>3,31</sup> This is surprising considering the probable importance of the monovalent copper oxidation state in oxygenase and oxidase chemistry.<sup>3–5,32</sup> Data with ligands of less physiological relevance are available. Structures of Cu(I) complexes with sterically unencumbered monodentate ligands are frequently tetrahedral.<sup>33</sup> An example with a nitrogenous ligand is  $(\text{pyridine})_4\text{Cu}^+\text{ClO}_4^-$ ,<sup>34</sup> here the average Cu–N bond distance is 2.05 (1) Å. It appears that the Cu–N bond distance decreases with decreasing coordination number. In  $(2\text{-picoline})_3\text{Cu}^+\text{ClO}_4^-$ ,<sup>35</sup> the Cu–N distances are 1.98, 1.97, and 2.02 Å, and the coordination geometry approaches trigonal planar. The four-coordinate mononuclear complex  $\text{HBpz}_3\text{Cu}(\text{CO})$ <sup>25</sup> approaches a  $C_{3v}$  structure with Cu–N distances of 2.039 (4)–2.059 (3) Å. These distances are longer than the average bond distances found for the Cu–N (terminal) interactions in  $[\text{HBpz}_3\text{Cu}]_2$  (1.947 (2) Å) and in  $[\text{HB}(\text{Me}_2\text{pz})_3\text{Cu}]_2$  (1.986 (3) Å). Including the bridging or semibridging Cu–N interactions in the latter two averages lead to larger values of 2.093 and 2.183 Å, respectively.

A number of examples are known where ligands capable of bridging lead to polynuclear cluster structures with relatively short Cu(I)–Cu(I) distances.<sup>31,33</sup> Cases with nitrogenous ligands are  $[(\text{dimethyltriazenyl})\text{Cu}]_4$ <sup>36</sup> and  $[(\text{diphenyltriazenyl})\text{Cu}]_2$ .<sup>37</sup> The former structure consists of a

rhombus of copper atoms (nearest neighbor Cu–Cu distances range from 2.64 (1) to 2.68 (1) Å), while the latter contains a pair of copper atoms (Cu–Cu = 2.451 (8) Å). In both structures, the bidentate triazene ligands span pairs of copper atoms, with Cu–N (average) equal to 1.87 (3) Å in the former and 1.92 (2) Å in the latter. In both cases the immediate coordination geometry about the metal, neglecting Cu–Cu interaction, is approximately linear two-coordinate, which may explain the shortness of the Cu–N distances. The metal–metal distances are comparable to those found in  $[\text{HBpz}_3\text{Cu}]_2$ , 2.660 (1) Å, and in  $[\text{HB}(\text{Me}_2\text{pz})_3\text{Cu}]_2$ , 2.506 (1) Å.

The foregoing discussion indicates that neither the magnitude of the terminal copper–nitrogen interactions nor the presence of close copper–copper contacts in  $[\text{HBpz}_3\text{Cu}]_2$  and  $[\text{HB}(\text{Me}_2\text{pz})_3\text{Cu}]_2$  is unexpected or unusual for a Cu(I) complex. What is unusual is the straddling of the metals by the pyrazolylborate ligands, the engagement of pyrazole units in bridging interactions, and the stereochemical nonrigidity of these systems. The first phenomenon is best rationalized in terms of a preference of Cu(I) to achieve a tetrahedral or trigonal planar coordination geometry. The most suitable (though still distorted) bond angles are only available when the hydrotris(pyrazolyl)borate ligands bridge the copper atoms. This preference can apparently be overcome by steric factors in  $[\text{HB}(\text{Me}_2\text{pz})_3\text{Cu}]_2$ , which is extensively dissociated in solution.

The presence of bridging heterocyclic ligands in  $[\text{HBpz}_3\text{Cu}]_2$  appears to reflect both preference in copper coordination geometry as well as electron deficiency. Formally, each copper possesses a 16-electron valence configuration, and three-center two-electron bridge bonds together with close copper–copper contacts are not unexpected.<sup>38,39</sup> The reason bridging by a heterocyclic ligand is observed in the present case, but is usually not observed, apparently also reflects the anionic charge of the pyrazolylborate ligand. Cu(I) complexes with typical neutrally charged heterocyclic ligands would be cationic. In many of these cases the accompanying counterion, e.g., a halide, could satisfy any electron deficiency by coordinating to the copper, and multicenter bonding would not be observed. In the case of  $[\text{HB}(\text{Me}_2\text{pz})_3\text{Cu}]_2$ , the highly unsymmetrical bridging appears to result from steric interactions as well as from the fact that the structures are relatively “floppy”.

In all probability, the potential energy surfaces describing major excursions from the ground state bonding geometries are relatively flat for both copper pyrazolylborates. The dissociation of  $[\text{HB}(\text{Me}_2\text{pz})_3\text{Cu}]_2$  in solution and the rapid interchange of bridge and terminal pyrazole ligands in  $[\text{HBpz}_3\text{Cu}]_2$  are indications of this. The latter process is permutationally similar to bridge–terminal ligand interchange processes observed for metal carbonyls, isocyanides, and nitrosyls.<sup>40</sup> By NMR, we cannot distinguish between rapid dissociation–reassociation of the dimer and intramolecular rearrangement. However, in reference to the latter process, it should be noted that the structures of  $[\text{HBpz}_3\text{Cu}]_2$  and  $[\text{HB}(\text{Me}_2\text{pz})_3\text{Cu}]_2$  are related by rotation of the tridentate ligand about the B–H bond axis and rotation of the pyrazole rings about the B–N bond axes. Hence, the solid-state structure of the methylated compound represents a plausible intermediate species along the reaction coordinate for nondissociative interchange of bridging and terminal pyrazole rings in  $[\text{HBpz}_3\text{Cu}]_2$ . The situation is analogous to the apparent role of “semibridging” CO groups in polynuclear nonrigid metal carbonyl compounds.<sup>41</sup> The process may also be operationally similar to polytopal isomerizations observed in mononuclear pyrazolylborate complexes.<sup>42</sup>

The present results and discussion suggest a number of



characteristics for Cu(I) ions present in polyimidazole protein binding sites. These include high conformational mobility and variable coordination geometry. In addition, the occurrence of copper atoms in pairs (which facilitates two electron redox processes)<sup>3,5</sup> should not be unexpected, and it is conceivable that the pairing is accompanied by short copper-copper contacts and bridging by imidazole ligands.

**Acknowledgments.** We are grateful to the National Science Foundation (T.J.M., GP-30623X and GP-43642X), the National Institutes of Health (J.A.I., HL-13157), and the Paint Research Institute (T.J.M.) for generous support of this research.

**Supplementary Material Available:** a listing of calculated positions of H atoms in [HBpz<sub>3</sub>Cu]<sub>2</sub> (Table II) and [HB(Me<sub>2</sub>pz)<sub>3</sub>Cu]<sub>2</sub> (Table V), root mean square of amplitudes of vibration in [HBpz<sub>3</sub>Cu]<sub>2</sub> (Table III) and [HB(Me<sub>2</sub>pz)<sub>3</sub>Cu]<sub>2</sub> (Table VI), and structure factor tables (40 pages). Ordering information is given on any current masthead page.

## References and Notes

- (1) Laboratorio Stereochimica CNR, Firenze, Italy.
- (2) Fellow of the Alfred P. Sloan Foundation.
- (3) (a) R. Osterberg, *Coord. Chem. Rev.*, **12**, 309 (1974); (b) J. Peisach, P. Aisen, and W. E. Blumberg, Ed., "The Biochemistry of Copper", Academic Press, New York, N.Y., 1966; (c) B. L. Vallee and W. E. C. Wacker, "The Proteins", 2nd ed., Vol. V, H. Neurath, Ed., Academic Press, New York, N.Y., 1970.
- (4) (a) F. Ghirelli, Ed., "Physiology and Biochemistry of Haemocyanins", Academic Press, New York, N.Y., 1966; (b) K. E. van Holde and E. F. J. van Bruggen in "Subunits in Biological Systems", S. N. Timasheff and G. D. Fasman, Ed., Marcel Dekker, New York, N.Y., 1971, p. 1; (c) P. Lontie and R. Witters in "Inorganic Biochemistry", Vol. 1, G. L. Eichorn, Ed., Elsevier, Amsterdam, 1973, Chapter 12.
- (5) (a) H. S. Mason, *Annu. Rev. Biochem.*, **34**, 595 (1965); (b) reference 3b, part 5; (c) A. J. M. Schoot Uiterkamp and H. S. Mason, *Proc. Nat. Acad. Sci. U.S.A.*, **70**, 993 (1973), and references therein; (d) R. Malkin in ref 4c, Chapter 21; (e) W. H. Vanneste and A. Zuberbuhler in "Molecular Mechanisms of Oxygen Activation", O. Hayaishi, Ed., Academic Press, New York, N.Y., 1974, Chapter 9.
- (6) J. S. Loehr, T. B. Freedman, and T. M. Loehr, *Biochem. Biophys. Res. Commun.*, **56**, 510 (1974).
- (7) B. Salvato, A. Ghirelli-Magaldi, and F. Ghirelli, *Biochemistry*, **13**, 4778 (1974).
- (8) (a) J. O. Alben, L. Yen, and N. J. Farrier, *J. Am. Chem. Soc.*, **92**, 4475 (1970); (b) J. O. Alben and L. Y. Fager, *Biochemistry*, **11**, 4786 (1972).
- (9) (a) M. I. Bruce, *J. Organomet. Chem.*, **44**, 209 (1972); (b) F. A. Cotton and T. J. Marks, *J. Am. Chem. Soc.*, **92**, 5114 (1970).
- (10) A. Liljas, K. K. Kannan, P. C. Bergsten, I. Waara, K. Fridborg, B. Strandberg, U. Carlborn, L. Jarup, L. Lovgren, and M. Petef, *Nature (London)*, **235**, 131 (1972).
- (11) K. K. Kannan, B. Notstrand, K. Fridborg, S. Lovgren, A. Ohlsson, and M. Petef, *Proc. Nat. Acad. Sci. U.S.A.*, **72**, 51 (1975).
- (12) T. L. Blundell, G. G. Dobson, E. J. Dodson, D. C. Hodgkin, and M. Vijayan, *Recent Prog. Horm. Res.*, **27**, 1 (1971).
- (13) J. S. Richardson, K. A. Thomas, B. H. Rubin, and D. C. Richardson, *Proc. Nat. Acad. Sci. U.S.A.*, **72**, 1349 (1975).
- (14) W. N. Lipscomb, J. A. Hartsuck, F. A. Quioco, and G. N. Reeke, Jr., *Proc. Nat. Acad. Sci. U.S.A.*, **64**, 28 (1969).
- (15) W. N. Lipscomb, J. A. Hartsuck, G. N. Reeke, F. A. Quioco, P. H. Bethge, M. L. Ludwig, T. A. Stertz, H. Muirhead, and J. C. Coppola, *Brookhaven Symp. Biol.*, **No. 21**, 24 (1968).
- (16) (a) S. Trofimenko, *Acc. Chem. Res.*, **4**, 17 (1971); (b) *Chem. Rev.*, **72**, 497 (1972).
- (17) M. I. Bruce and A. P. P. Ostaszewski, *J. Chem. Soc., Dalton Trans.*, 2433 (1973).
- (18) C. S. Arcus, J. L. Wilkinson, C. Mealli, T. J. Markes, and J. A. Ibers, *J. Am. Chem. Soc.*, **96**, 7564 (1974) (preliminary communication).
- (19) T. J. Marks, C. S. Arcus, J. L. Wilkinson, and P. L. Dedert, unpublished results.
- (20) (a) S. Trofimenko, *J. Am. Chem. Soc.*, **89**, 3170 (1967); (b) *Inorg. Synth.*, **12**, 99 (1970).
- (21) D. F. Shriver, "The Manipulation of Air-Sensitive Compounds", McGraw-Hill, New York, N.Y., 1969, p. 159.
- (22) P. W. R. Corfield, R. J. Doedens, and J. A. Ibers, *Inorg. Chem.*, **6**, 197 (1967).
- (23) B. A. Averill, T. Herskovitz, R. H. Holm, and J. A. Ibers, *J. Am. Chem. Soc.*, **95**, 3423 (1973).
- (24) See paragraph at end of paper regarding supplementary material.
- (25) M. R. Churchill, B. G. DeBoer, F. J. Rotella, O. M. Abusalah, and M. I. Bruce, *Inorg. Chem.*, **14**, 2051 (1975). We thank Professor Churchill for making his data available to us prior to publication.
- (26) M. R. Churchill, K. Gold, and C. E. Maw, Jr., *Inorg. Chem.*, **9**, 1597 (1970).
- (27) F. A. Cotton, B. A. Frenz, and A. Shaver, *Inorg. Chim. Acta*, **7**, 161 (1973).
- (28) B. W. Davies and N. C. Payne, *Inorg. Chem.*, **13**, 1843 (1974).
- (29) G. Avitabile, P. Ganis, and M. Nemiroff, *Acta Crystallogr., Sect. B*, **27**, 725 (1971).
- (30) See C. A. Kosky, P. Ganis, and G. Avitabile, *Acta Crystallogr., Sect. B*, **27**, 1859 (1971), for the structure of H<sub>2</sub>B(3,5-Me<sub>2</sub>pz)<sub>2</sub>Mo(CO)<sub>2</sub>( $\eta^3$ -C<sub>3</sub>H<sub>5</sub>).
- (31) (a) W. E. Hatfield and R. Whyman, *Transition Metal Chem.*, **5**, 47 (1969); (b) F. H. Jardine, *Adv. Inorg. Chem. Radiochem.*, **17**, 115 (1975).
- (32) The paucity of data probably reflects both the air-sensitivity of the Cu(I) complexes (as opposed to stability of those of Cu(II)) as well as the propensity for some Cu(I) complexes to disproportionate to Cu(0) and Cu(II).<sup>33</sup>
- (33) F. A. Cotton and G. Wilkinson, "Advanced Inorganic Chemistry", 3rd ed., Interscience, New York, N.Y., 1972, p. 905.
- (34) A. H. Lewin, R. J. Michl, P. Ganis, U. Lepore, and G. Avitabile, *Chem. Commun.*, 1400 (1971).
- (35) A. H. Lewin, R. J. Michl, P. Ganis, and U. Lepore, *J. Chem. Soc., Chem. Commun.*, 661 (1972).
- (36) J. E. O'Connor, G. A. Janusonis, and E. R. Corey, *Chem. Commun.*, 445 (1968).
- (37) I. D. Brown and J. D. Dunitz, *Acta Crystallogr.*, **14**, 480 (1961).
- (38) R. Mason and D. M. P. Mingos, *J. Organomet. Chem.*, **50**, 53 (1973).
- (39) We find by cryoscopy that electron sufficient complexes such as HBpz<sub>3</sub>CuPR<sub>3</sub> are unassociated in solution.<sup>19</sup>
- (40) (a) F. A. Cotton and R. D. Adams in "Dynamic Nuclear Magnetic Resonance Spectroscopy", L. M. Jackson and F. A. Cotton, Academic Press, New York, N.Y., 1975, Chapter 12; (b) F. A. Cotton, *Bull. Soc. Chim. Fr.*, 2588 (1973); (c) R. M. Kirchner, T. J. Marks, J. S. Kristoff, and J. A. Ibers, *J. Am. Chem. Soc.*, **95**, 6602 (1973).
- (41) F. A. Cotton and J. M. Troup, *J. Am. Chem. Soc.*, **96**, 1233 (1974).
- (42) H. C. Clark and L. E. Manzer, *Inorg. Chem.*, 1996 (1974).